



Molecular Crystals and Liquid Crystals

Publication details, including instructions for authors and subscription information:

<http://www.tandfonline.com/loi/gmcl20>

Polarization Optics of Microstructured Liquid Crystal Fibers

Tomasz R. Woliński^a, Piotr Lesiak^a, Andrzej W. Domański^a, Sławomir Ertman^a, Katarzyna Szaniawska^a, Roman Dąbrowski^b, Edward Nowinowski-Kruszelnicki^b & Jan Wójcik^c

^a Faculty of Physics, Warsaw University of Technology, Koszykowa, Warszawa, Poland

^b Military University of Technology, Warszawa, Poland

^c Maria Curie Skłodowska University, Lublin, Poland

Version of record first published: 22 Sep 2006

To cite this article: Tomasz R. Woliński, Piotr Lesiak, Andrzej W. Domański, Sławomir Ertman, Katarzyna Szaniawska, Roman Dąbrowski, Edward Nowinowski-Kruszelnicki & Jan Wójcik (2006): Polarization Optics of Microstructured Liquid Crystal Fibers, *Molecular Crystals and Liquid Crystals*, 454:1, 325/[727]-342/[744]

To link to this article: <http://dx.doi.org/10.1080/15421400600656012>

PLEASE SCROLL DOWN FOR ARTICLE

Full terms and conditions of use: <http://www.tandfonline.com/page/terms-and-conditions>

This article may be used for research, teaching, and private study purposes. Any substantial or systematic reproduction, redistribution, reselling, loan,

sub-licensing, systematic supply, or distribution in any form to anyone is expressly forbidden.

The publisher does not give any warranty express or implied or make any representation that the contents will be complete or accurate or up to date. The accuracy of any instructions, formulae, and drug doses should be independently verified with primary sources. The publisher shall not be liable for any loss, actions, claims, proceedings, demand, or costs or damages whatsoever or howsoever caused arising directly or indirectly in connection with or arising out of the use of this material.



Polarization Optics of Microstructured Liquid Crystal Fibers

Tomasz R. Woliński

Piotr Lesiak

Andrzej W. Domański

Sławomir Ertman

Katarzyna Szaniawska

Faculty of Physics, Warsaw University of Technology,
Koszykowa, Warszawa, Poland

Roman Dąbrowski

Edward Nowinowski-Kruszelnicki

Military University of Technology, Warszawa, Poland

Jan Wójcik

Maria Curie Skłodowska University, Lublin, Poland

The present paper discusses polarization phenomena occurring in microstructured liquid crystal fibers and in particular solid-core photonic crystal fibers infiltrated with liquid crystals. We report on the latest experimental polarization characteristics of microstructured photonic crystal fibers filled with prototype nematic liquid crystal guest materials characterized by either extremely low (of the order ~ 0.05) or medium (of the order ~ 0.2) material birefringence. Due to anisotropic properties of the microstructured liquid crystal fibers switching between different guiding mechanisms as well as electrically and temperature-induced tuning of light propagation have been demonstrated. These preliminary results hold great potential for both fiber-optic sensing and in-fiber polarization mode dispersion control and compensation.

Keywords: microstructured liquid crystal fiber; polarization; polarization mode dispersion

The work was supported by the Polish Ministry of Science and Education under the grant 3T10C 016 28.

Address correspondence to Tomasz R. Woliński, Faculty of Physics, Warsaw University of Technology, Koszykowa 75, 00-662 Warszawa, Poland. E-mail: wolinski@if.pw.edu.pl

INTRODUCTION

Anisotropic optical fibers that exhibit particular polarization properties have been extensively investigated for over the last two decades [1]. This includes also an elliptical liquid crystal-core fiber infiltrated with a nematic liquid crystal (LC) mixture characterized by extremely low values of refractive indices can exhibits single-polarization behavior at a certain temperature range [2]. Recently, there has been a great interest in microstructured photonic crystals fibers (PCFs) and particularly in yet more advanced micro-structures known as microstructured (photonic) liquid crystal fibers [3,4]. The microstructured liquid crystal fiber consisting of a PCF filled with a LC benefits from a combination of a passive PCF host structure and an “active” LC guest material being responsible for diversity of new and uncommon properties.

In optical communication, polarization mode dispersion (PMD) is regarded as a major limitation in optical transmission systems in general and an ultimate limitation for ultra-high speed single channel systems based on standard single mode fibers. Polarization mode dispersion is usually expressed by differential group delay (DGD) over the length of the fiber $\Delta\tau/L$. Both values: PMD and modal birefringence $\Delta\beta$ are the most important parameters characterizing birefringent fibers and are interrelated according to the formula [5]:

$$\frac{\Delta\tau}{L} = \frac{d(\Delta\beta)}{d\omega} = \frac{1}{c} \left(\Delta n_{\text{eff}} + \omega \frac{d\Delta n_{\text{eff}}}{d\omega} \right) \quad (1)$$

where $\Delta\tau/L$ is usually expressed in units of picoseconds per kilometer of fiber length, Δn_{eff} is the differential effective index of refraction for the slow and fast polarization modes, and $\omega = 2\pi c/\lambda$ is the angular frequency of light.

In highly birefringent (HB) fibers with stress-induced birefringence (e.g. bow-tie fibers [1]) in which birefringence is caused by stress applying parts introduced in cladding close to the core region of the fiber, Δn_{eff} is nearly wavelength independent and the chromatic dispersion of the modal birefringence is negligible. Hence for this type of fibers measurements of birefringence and PMD are equivalent.

$$\frac{\Delta\tau}{L} \cong \frac{1}{c} \Delta n_{\text{eff}} = \frac{\lambda}{L_B c} \quad (2)$$

where L_B is beat length expressed as:

$$L_B = \frac{2\pi}{|\beta_y - \beta_x|} \quad (3)$$

and responsible for phase difference changes along the HB fiber. The spatial period L_B of these changes reflects the modulation in the polarization states along the fiber. Linearly polarized light coupled into the HB fiber with plane of polarization directed at the angle of 45 degrees between both axes of birefringence excites both field components HE_{11}^x and HE_{11}^y of the fundamental HE_{11} fiber mode and as these two orthogonal mode components are characterized by different propagation constants β_x and β_y , they run into and out of phase at a rate determined by the birefringence of the HB fiber producing at the same time a periodic variation in the transmitted polarization state from linear through elliptic to circular and back again.

MICROSTRUCTURED LIQUID CRYSTAL FIBERS

To investigate temperature and electrical field effects on propagation and polarization properties of PLCFs we used a prototype microstructured fiber manufactured at Maria Curie Skłodowska University (MCSU), Lublin (Poland) and also commercially available highly birefringent PCF of the type PM-1550-01 manufactured by Blaze-photonics (UK). The cross sections of both fibers are shown in Figure 1.

The MCSU photonic crystal fiber has a solid core with a diameter of $10\mu\text{m}$ is surrounded by nine rings of the holes characterized by diameters and hole spacing of $4.8\mu\text{m}$ and $6.5\mu\text{m}$, respectively and right one a solid elliptical core with a diameter of $3.1/3.6\mu\text{m}$ is created by

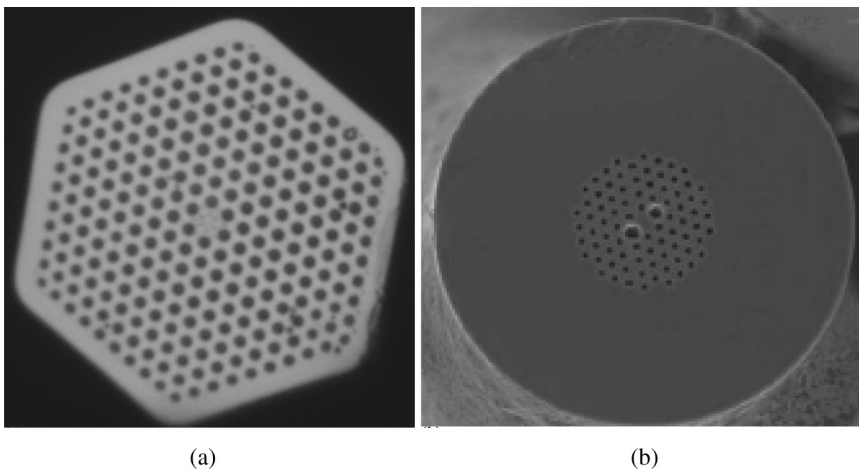


FIGURE 1 a) MCSU 1023 PCF; b) HB PCF of the type PM-1550-01.

TABLE 1 Birefringence of Nematic LCs used as Guest Materials of PLCF (22°C, $\lambda = 589\text{ cm}$)

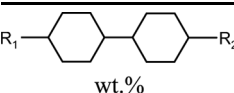
LC	Ordinary index n_o	Extraordinary index n_e	Birefringence Δn	Clearing temperature [°C]	Dielectric anisotropy
PCB	1.533	1.726	0.20	33	16.1
1550	1.461	1.522	0.06	78	3.2

different diameters of holes in orthogonal directions $2.2\mu\text{m}$ and $4.5\mu\text{m}$, respectively. A non-circular core combined with the large air-glass refractive index step in this photonic crystal fiber creates strong form birefringence. Both microstructured PCFs were used as a host structure, while LCs played a role of guest materials. In the MCSU fiber, cladding region of the PCF structure was infiltrated with a nematic mixture whereas in the PM-1550-01 HB PCF only two large holes were filled with a liquid crystal.

As a guest material we used two different nematic LCs: a typical nematic pentylo-cyano-biphenyl, PCB and a prototype nematic mixture cat. no. 1550, both manufactured at Military University of Technology in Warsaw (Table 1). The 1550 liquid crystalline mixture ($n_o = 1.461$, $n_e = 1.522$ at 22°C, $\lambda = 589\text{ nm}$) was composed of alkyl 4-trans-(4-trans-alkylcyclohexyl) cyclohexylcarbonates (Table 2). They were synthesized according to the route shown in Figure 2 presented in details elsewhere [6]. Their optical properties were described in [7].

Temperature dependence of refractive indices of the 1550 nematic LC (Fig. 3) shows that there is a specific temperature region of the nematic phase (close to 33°C, at 633 nm) in which its ordinary refractive index n_o is below the refractive index of the fused silica $n_{\text{silica}} = 1.458$ (at $\lambda = 589\text{ nm}$) while its extraordinary index is still higher than n_{silica} .

TABLE 2 Composition and Mesomorphic Properties of the 1550 LC Mixture

 wt. %	R ₁	R ₂	Crystal-nematic phase transition temperature (°C)	Nematic-isotropic phase transition temperature (°C)
23.93	C ₃ H ₇	OCOOC ₂ H ₅	59.4	71.4
18.24	C ₅ H ₁₁	OCOCH ₃	70.5	95.0
34.55	C ₅ H ₁₁	OCOOC ₂ H ₅	54.8	85.0
23.28	C ₃ H ₇	CN	57.0	79.7

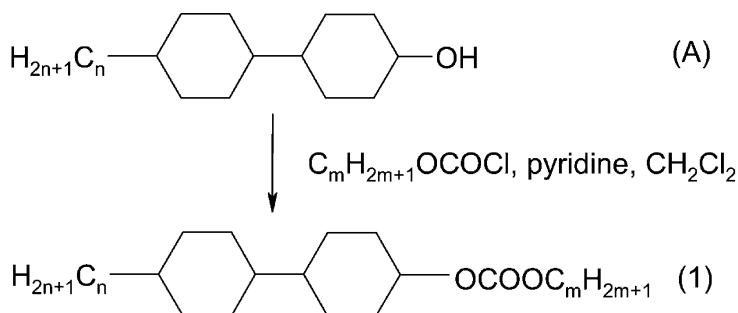


FIGURE 2 Route of synthesis alkyl trans-4-(trans-4-alkylcyclohexyl) cyclohexylcarbonates.

Propagation properties and especially the photonic band gap (PBG) effect strongly depend on molecular alignment within the host PCF holes as it is schematically drawn in Figure 4. The liquid crystalline molecular arrangements (director field configurations) in the cladding cylindrical micro holes are determined by surface glass anchoring

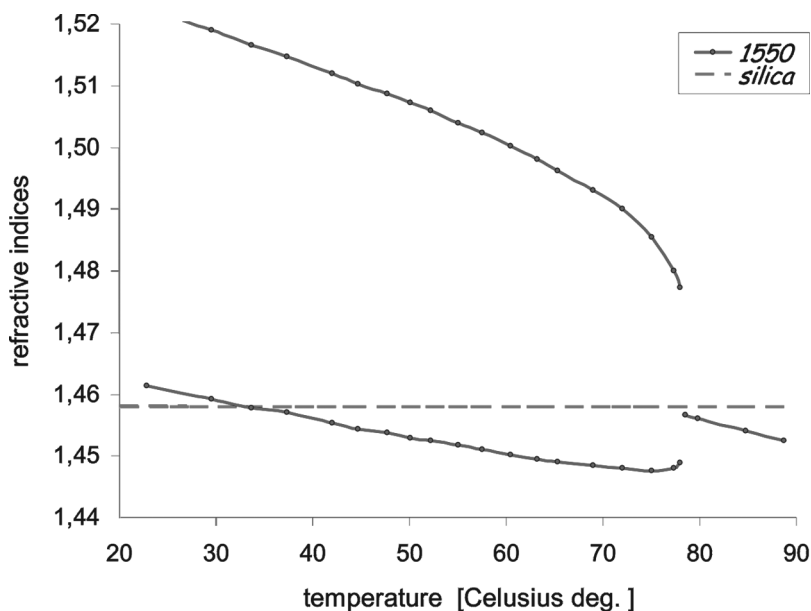


FIGURE 3 Refractive indices as a function of temperature for the 1550 LC mixture.

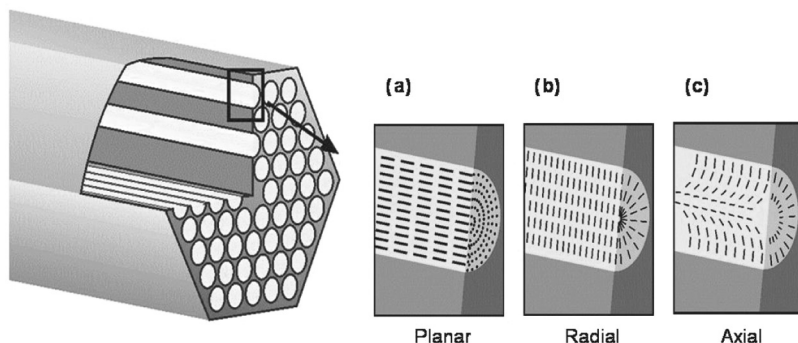


FIGURE 4 Molecular arrangements within the cylindrical holes of PCF cladding region: (a) planar, (b) radial, and (c) axial.

conditions. Generally, three types of the LC molecular alignment inside the fibers holes are possible: planar (Fig. 4a), radial (homeotropic) (Fig. 4b), and a combination of two previous structures, the so-called radial-escaped or axial geometry (Fig. 4c). Due to flow-induced orientation during the filling process both planar and axial alignments dominate over the radial alignment.

The arrangement of liquid crystal molecules within the cylindrical holes of the PCF cladding region is crucial to understanding of guidance mechanisms of the PLCF. We have carefully investigated liquid crystalline molecular alignment on fused silica capillaries filled with both liquid crystals. Inner diameter of the capillaries matched the dimensions of the host PCF holes whereas internal structure of the LC-capillaries analysis was based on reconstruction of the 3-dimensions refractive index distribution in optical phase microelements. The automated tomographic microinterferometer technique was applied similarly to our former work on elliptical-core liquid crystal fiber [8]. It appeared that light polarized along fiber axis detects extraordinary refractive index of the infilling LC confirming the fact that the LC molecules are predominantly oriented along the fiber axis.

TUNING OF THE WAVELENGTH IN PLCFS

Propagation properties and especially the photonic band gap (PBG) effect strongly depend on features of liquid crystals used as filling materials. Molecular alignment within the host PCF holes is crucial issue in this consideration. The director field configurations in the cladding cylindrical LC-holes are determined by surface glass anchoring conditions. It seems that planar and axial alignments are

dominated over the radial alignment due to flow-induced orientation during the filling process.

In experimental investigation we used a ~ 50 cm long photonic crystal host fiber in which only ~ 10 mm long section was filled with the guest nematic LC by using the capillary forces. The input light from a broad-band source was coupled into an empty section of the PCF. The terminal part of the PCF filled with LC created the PLCF under investigation was placed between electrodes. The electrodes were plugged to a high-voltage source, which allowed controlling both voltage from 0 V to 1000 V and frequency from 200 Hz to 2 kHz. The optical signal from the output of the PLCF was analyzed by the Ocean Optics fiber optic spectrometer and the PLCF was thermally controlled by a temperature stabilization device.

Thermal Effects

Guiding of the light in a PCF is governed by one of two principal mechanisms responsible for light trapping within the fiber core. One of them is an index guiding mechanism based on the total internal reflection (TIR) phenomenon, which is well known and similar to the wave guiding within a conventional fiber. The other mechanism is known as a PBG effect that occurs when the effective reflective index of the cladding region is larger than the index of the core region. In this case the propagation mechanism relies on the confinement of the light trapped inside of the core.

The PCF used as a host structure is a typical solid-core holey fiber with an index guiding mechanism. However, the liquid crystalline material placed into the holes of the cladding region influences not only the properties of the light propagation, but can also change the guiding mechanism.

The guiding mechanism of the PLCF depends on the effective refractive index of the nematic LC that strongly depends on the ambient temperature and the molecular alignment. Due to flow-induced orientation during the filling process of the PLCF, planar and axial molecular alignments dominate over the radial geometry. It means that the propagating light experiences the effective refractive index that is close to the ordinary refractive index of the guest nematic LC [9,10].

Due to the unusual ordinary refractive index temperature dependence of the 1550 nematic mixture, switching between two propagation mechanisms was observed. Spectral characteristic for two guiding mechanisms are presented in Figure 5. Figure 5a shows temperature influence on PBGs positions that are shifted towards the shorter wavelengths (blue shift) with an increase of temperature.

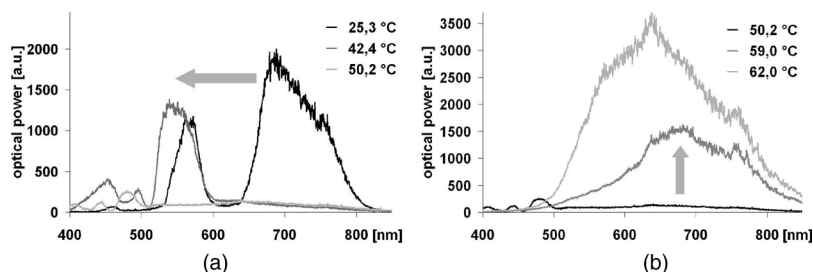


FIGURE 5 Transmission spectra of the PLCF (1550 LC). In Figure 5A light is guided by the PBG effect, and a temperature increase induces the blue shift (n_{LC} is higher than n_{silica}). In Figure 5b, the whole launched spectrum is observed (TIR effect); optical power increases with temperature (n_{LC} is lower than n_{silica}).

The transmitted spectrum fades into the lack of the propagation when the average refractive index of the cladding region is close to the silica core index. When the PLCF is heated further on propagation appears again, but now with the index guiding mechanism allowing for transmission of the full spectrum of the light source coupled into the fiber (Fig. 5b). Consequently, the PLCF becomes a typical index-guiding PCF, and light trapping in the core increases with temperature.

In order to obtain results, which enable us to demonstrate a difference in guiding mechanisms of the PLCF close to the nematic-isotropic phase transition we used PCB that is characterized by higher values of both ordinary and extraordinary refractive indices in comparison with silica glass. Figure 6 presents the transmission characteristics of the PLCF with PCB below (a) and above (b) nematic-isotropic phase transition temperature and demonstrates differences in the optical power transmitted in these two cases. For the nematic phase of PCB temperature-tunable photonic band gaps are possible. The output optical power for the isotropic phase dramatically increases in comparison with the transmission for the nematic phase. This behavior can be attributed to disappearance of molecular long-range orientation order in isotropic phase, and in consequence is responsible for lower attenuation. Moreover the wavelength shift direction is determined by character of temperature dependence of PCB. For nematic phase of PCB the wavelengths moves towards longer wavelength (n_o increase with temperature), while for isotropic phase the blue shift is observed (n_{iso} decrease with temperature). Thus every LC host cylinder in the PLCF cladding becomes a waveguide, and light propagates with the LC medium. As a result the whole launched spectrum can be guided

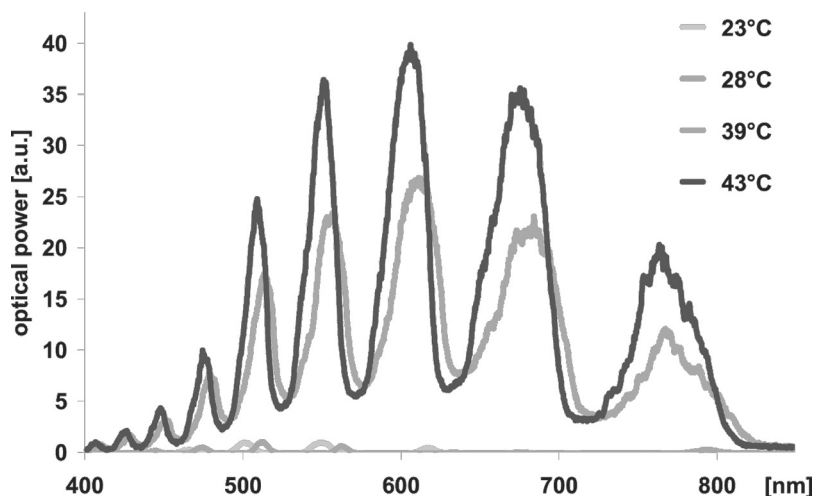


FIGURE 6 Transmission spectra of the PLCF with PCB in two cases: below and above the nematic-isotropic phase transition.

by LC guest medium while the selective wavelengths still propagate within the PLCF core by the PBG effect.

Electrical Tuning of Photonic Band Gaps

For the PCF filled with PCB, applied voltage increases the optical power transmitted within the PLCF, but positions of photonic band gaps are different than in the off-voltage state (Fig. 7). Hence, electrical tuning of PLCFs allows for switching between two different positions of PBGs which depends on ordinary refractive index of LC in off-voltage state and extraordinary index in the high-voltage state. In our case we observed shifted PBGs that appear at certain value of voltage. Any change in the propagated wavelength is obtained due to the LC molecular reorientation effect induced by an external electrical field. Below threshold voltage, the propagation is governed by the ordinary refractive index within the LC capillary, however above a critical voltage, the reorientation effect occurs and propagation observes the LC extraordinary index. As a result different guidance conditions are met in and consequently the band gaps switching is obtained.

However, further voltage increases (as observed in Fig. 7) induce electrically-tuned transmission of the photonic band gaps in the PLCFs. This effect strongly depends on the operating wavelength.

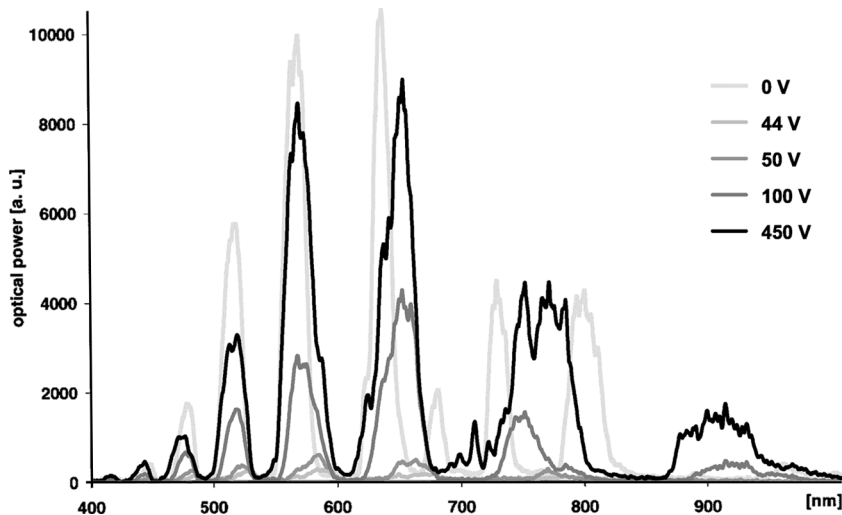


FIGURE 7 Electrical tuning of PBG's position in the PLCF filled with PCB.

POLARIZATION PROPERTIES OF THE PLCF

The experimental setup for investigation of propagation and polarization properties of the PLCFs is shown in Figure 8. We used ~50 cm long photonic crystal host fibers in which only ~10 mm long section of MCSU PCF structure [11] and ~10–70 mm of HB PM-1550-01 PCF in which only two big holes on both sides of the fiber core were

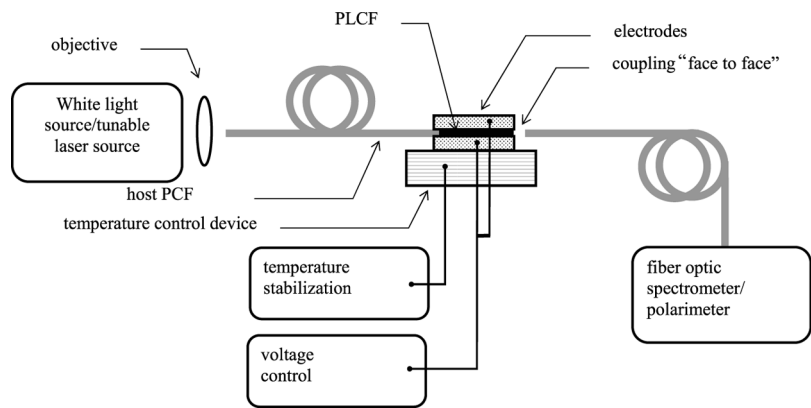


FIGURE 8 Experimental setup to investigate propagation and polarization properties of the PLCF.

filled with the guest nematic LC by using capillary forces. The input light from a broad-band source was coupled into an empty section of the MCSU PCF and the light from tunable laser source was coupled into an empty section of the HB PCF. The terminal part of the PCF filled with LC that created the PLCF under investigation was placed between electrodes. The electrodes were plugged to a high-voltage source, which allowed for controlling both voltage from 0 V to 1000 V and frequency from 200 Hz to 2 kHz. The optical signal from the output of the MCSU PLCF was analyzed by the Ocean Optics fiber optic spectrometer (both USB2000 and HR4000 models were used). The measurement apparatus included also a tunable laser source (*Tunics Plus CL*) operating at third optical window (spectral range 1500÷1640 nm) and a modular system for polarization analysis PAT 9000B polarimeter (*Tektronix*) to analyze output of the HB PLCF. The PLCFs were thermally controlled by a temperature stabilization device. The Jones Matrix Eigenanalysis method was selected for polarization mode dispersion (DGD) measurements [12].

The interesting effect was observed by changing the azimuth of the linearly polarized light launched into the MCSU PCF infiltrated with a high-birefringence nematic liquid crystal (cat. number 1294-1b) manufactured by Military University of Technology, Poland. Polarization of light was controlled by rotating the polarizer, which was placed between the broadband light source and the empty PCF. In the off-voltage state the PLCF was almost insensitive to polarization, however approx. 15% modulation of optical power has been observed when the polarizer was rotating. This behavior results generally from the fact that the light emitted by the white-light source used is partially polarized. In the high-voltage state, the PLCF becomes highly sensitive to the input linear polarization, as the reorientation of the LC molecules resulted in a high anisotropy of the PLCF cross-section. We have observed almost 98% modulation of the detected output intensity in function of the input polarization (Fig. 9). This suggests a single-polarization guiding of the PLCF similarly to the phenomenon observed by us in the elliptical-core LC fiber [2].

Birefringence in optical fibers arises from the difference in the effective indices (n_x - n_y) of the two orthogonal polarization modes of an optical fiber. In microstructured optical fibers (MOFs), strong birefringence has been demonstrated in fibers that incorporate elliptical air-holes [13], or an asymmetric distribution of air-holes in the fiber [14]. These types of birefringence can be easily modified by using LC mixture filled into air-holes.

Optical properties of the highly birefringent PM-1550-01 PCF (made by Blazephotonics) filled with the low-birefringence 1550 liquid

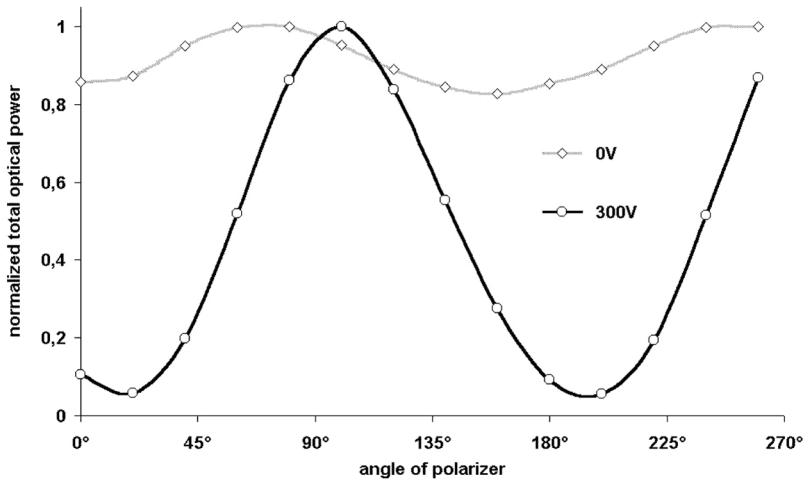


FIGURE 9 Modulation of optical power transmitted in the PLCF through rotating the polarizer. At the off-voltage stat only small changes of power are observed. At the higher voltage the PLCF becomes highly sensitive to polarization.

crystal mixture are generally similar to the properties of the MCSU PLCFs filled with the same LC. For temperature below 55°C (at 1550 nm) we observed band-gap guiding in the PM-1550-01 PLCF. Propagation wavelength dependence on ordinary refractive index of the infiltrated LC material (Fig. 10) suggests that the liquid crystalline

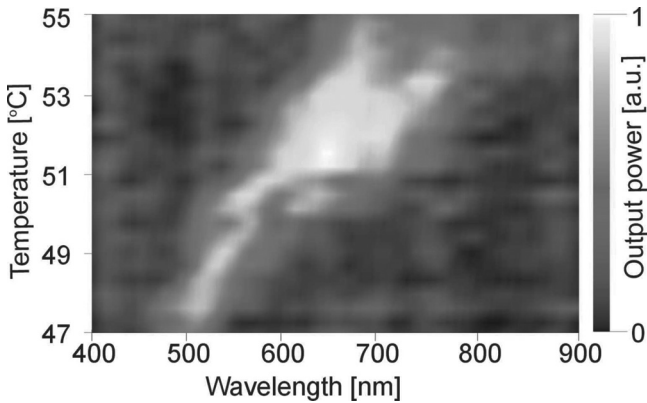


FIGURE 10 Influence of temperature on the optical spectrum after HB PLCF PM-1550-01.

molecules are planar oriented within the holes. It is possible to dynamically tune the propagating wavelength as a result of thermal dependence of the LC ordinary refractive index. In comparison to the previous measurements results we obtain only single polarization propagation at the band gap regime. This is a consequence of observed large out-radiation of the x -polarized mode into the LC region [15] and the effect is insensitive to number of filled holes.

For temperatures slightly below 55°C (single-mode propagation regime) influence of the electrical field was studied. It appeared that the external d.c. electrical field $\sim 1\text{V}/\mu\text{m}$ directed along the y -axis (Fig. 11) by inducing molecular reorientation within the holes switches the propagating light into the x -polarized mode. For the electrical field directed along the x -axis the x -polarized mode will “see” extraordinary

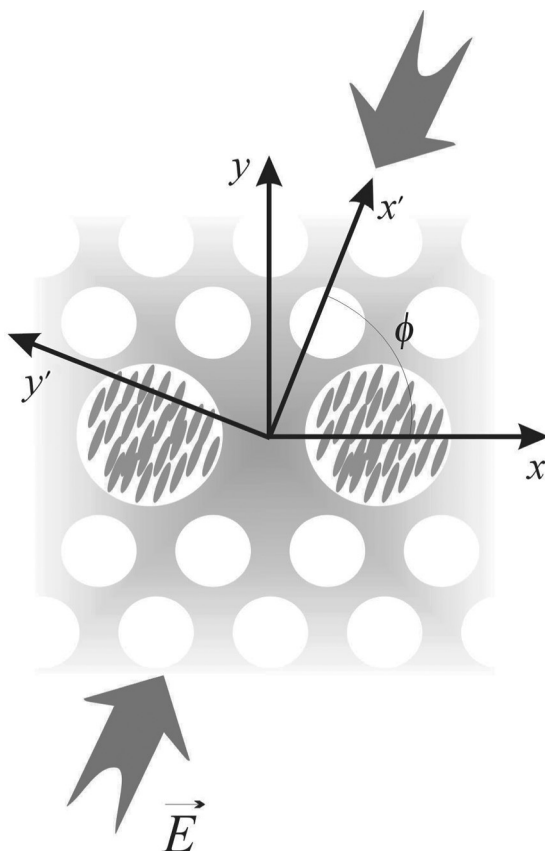


FIGURE 11 PLCF PM-1550-01 under external d.c. electric field.

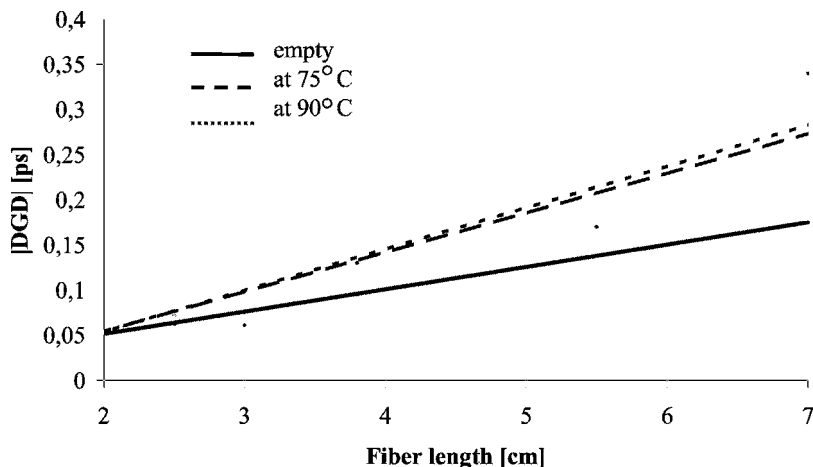


FIGURE 12 A comparison between decreases of the DGD in PCF and PLCF fibers at two different temperatures.

refractive index of the LC and will be out-radiated to the LC hole region.

For temperatures above 55°C the total internal reflection guiding mechanism in the PLCF PM-1550-01 was observed. Two orthogonal components of the basic mode have been propagated and in a consequence we could estimate the influence of LC on fiber birefringence by measuring differential group delay (DGD) in the fiber.

The HB PCF fiber produced by Blazephotonics is characterized by PMD equal to 2.75 ps/m. After infiltrated two large holes situated near the core with the 1559 LC (7 cm in length), the DGD value measured at 90°C decreased to 2.42 ps.

Compensation value of DGD in the measured fiber is explained in Figure 12. Solid line represents DGD in the empty PCF. However in the PLCF at two different temperatures (75 and 90 Celsius degree) the module of DGD changes more rapidly in the part of the HB PLCF fiber filled with LC. This can be explained in terms of reorientation of birefringence axes. Figure 13 shows both: temperature dependence of DGD in the PM-1550-01 PLCF and thermal dependence of the ordinary refractive index of the 1550 LC mixture used.

The clearing temperature of the 1550 LC mixture is equal to 80°C and this corresponds to a sudden drop of the DGD value at the nematic–isotropic phase transition. Changes in the DGD value around the 50÷80°C temperature range suggest that birefringence in the

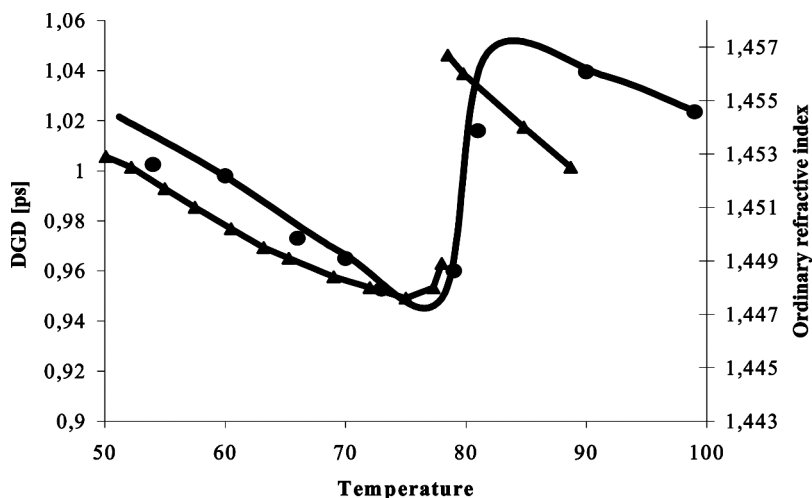


FIGURE 13 Temperature dependence of DGD and ordinary refractive index of the LC cat. no. 1550.

PLCF increased and the higher compensation of the DGD was observed. However, if the electrical field was switched on along the y -axis we have not observed any sudden drop of the DGD value around the clearing temperature (80°C) – see Figure 15.

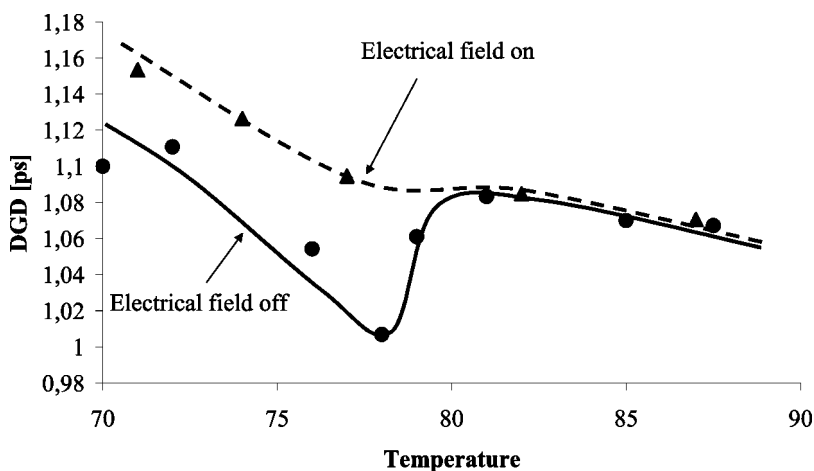


FIGURE 14 DGD as a function of temperature (PLCF = 3.8 cm).

DYNAMIC BIREFRINGENCE TUNING AND PMD COMPENSATION WITH PLCF

In general, partially coherent light during propagation through birefringent media becomes depolarized [15]. The depolarization depends on coherence of light characterized by the coherence length (ΔL), birefringence of the medium defined as Δn as well as on orientation of light beam versus fast and slow axes of the medium birefringence. The phenomenon occurs in each birefringent medium including highly birefringent optical fibers where $\Delta n = \Delta n_{\text{eff}}$ for both orthogonal polarization components of the fundamental HE_{11} fiber mode and as a consequence it is responsible for polarization mode dispersion (PMD) in optical fibers.

One of the potential applications of polarization effects in PLCFs is dynamic birefringence tuning that can be straightforwardly applied to in-line PMD compensation. Instead of using a compensator composed of two perpendicularly crossed and strained HB fibers we can use only one section of a photonic crystal fiber filled with a liquid crystal (Fig. 15). Introducing external electrodes we obtain a possibility of electrically-controlled LC molecular reorientation inside the holes of the PLCF and in the same way we have a control of the fiber birefringence.

In this case, only one simple matrix equation may be used [15]:

$$[S^{\text{out}}] = [D_c^*][M_{\text{PLCF}}][S^{\text{in}}] \quad (4)$$

where $S^{\text{in (out)}}$ is the input (output) spatial Stokes vector of the guided fiber mode [1], $[M_{\text{PLCF}}]$ is the Mueller matrix of the PLCF section, and



FIGURE 15 Photonic liquid crystal fiber (PLCF).

$[D_c]$ denotes the depolarization matrix, whose conjugated value is given by:

$$[D_c^*] = \begin{bmatrix} 1 & 0 & 0 & 0 \\ 0 & P_c^* & 0 & 0 \\ 0 & 0 & P_c^* & 0 \\ 0 & 0 & 0 & P_c^* \end{bmatrix} \quad (5)$$

with the conjugated degree of polarization P_c^* characterizing the light source used

$$P_c^* = \sqrt{1 - \frac{4 \left[1 - \exp \left(+ \frac{2\Delta n_{\text{eff}} L_{\text{PLCF}}}{\Delta L} \right) \right]}{\left(\frac{|u_1|}{|u_2|} + \frac{|u_2|}{|u_1|} \right)^2}} \quad (6)$$

where u_1, u_2 describe polarization components of the propagating fundamental HE_{11} fiber mode, L_{PLCF} denotes the length of the photonic liquid-crystal fiber, ΔL is the coherence length of the light source, and Δn_{eff} depends on refractive indices of LC and SiO_2 glass as well on distribution and size of the holes infilled with LC. Polarization diagram (Fig. 16) shows depolarization compensation for two different orientations of the LC molecules: $\Delta n_{\text{eff-1}}$ and $\Delta n_{\text{eff-2}}$ respectively.

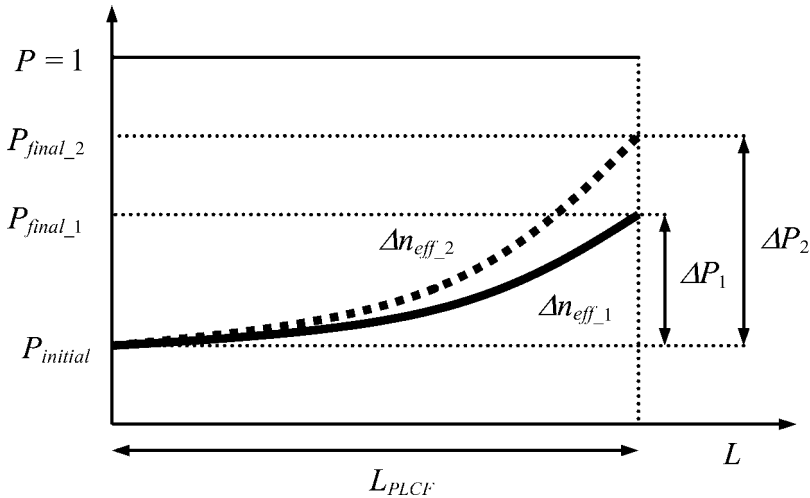


FIGURE 16 Polarization diagrams of the PLCF compensator.

CONCLUSIONS

Photonic crystal fibers infiltrated with liquid crystals exhibit unusual propagation and polarization properties. We have so far experimentally demonstrated: propagation within one PLCF governed by two guiding mechanisms: the photonic bandgap effect and the total internal reflection that can be easily tuned either by temperature or by external electric field. It appeared that PLCFs based on highly birefringent PCFs can guide only single polarization and are characterized by dynamically tuned birefringence as well as differential group delay. This can be directly applied to dynamic compensation of polarization mode dispersion and holds great potential in fiber-optic sensing.

REFERENCES

- [1] Wolinski, T. R. (2000). Polarimetric optical fibers and sensors. In: *Progress in Optics*, Wolf, E. (Ed.), Elsevier Science B.V.: North-Holland, Vol. XL, 1–75.
- [2] Wolinski, T. R., Szymanska, A., Nasilowski, T., Nowinowski, E., & Dabrowski, R. (2000). *Mol. Cryst. Liq. Cryst.*, 352, 361.
- [3] Szymanska, A. & Wolinski, T. R. (2002). *Mol. Cryst. Liq. Cryst.*, 375, 723.
- [4] Wolinski, T. R. (2003). Polarization phenomena in optical systems. In: *Encycl. of Opt. Engineering*, Diggers, R. (Ed.), M. Dekker: New York, 2150.
- [5] Wolinski, T. R. & Domanski, A. W. (2003). *Acta Physica Polonica A*, 103, 211.
- [6] Bock, W. J., Domański, A. W., & Wolinski, T. R. (1990). *Applied Optics.*, 29, 3484.
- [7] Schirmer, J., Kohns, P., Schmidt-Kaler, T., Muravski, A., Yakovenko, S., Bezborodov, V., Dabrowski, R., & Adomenas, P. (1997). *Mol. Cryst. Liq. Cryst.*, 307, 17.
- [8] Wolinski, T. R., Lesiak, P., Dabrowski, R., Kedzierski, J., & Nowinowski, E. (2004). *Mol. Cryst. Liq. Cryst.*, 421, 175.
- [9] Wolinski, T. R., Bondarczuk, K., Szaniawska, K., & Lesiak, P. (2004). *Proc. SPIE*, 5518, 232.
- [10] Wolinski, T. R. et al. (2005). *Opto-Electronics Review*, 13(2), 57.
- [11] Wojcik, J., Poturaj, K., Janoszczyk, B., Mergo, P., & Makara, M. (2003). *Proc. SPIE*, 5576, 102.
- [12] Heffner, B. L. (1992). *Photon. Technol. Lett.*, 4(9), 1066.
- [13] Ortigosa-Blanch, A., Knight, J. C., Wadsworth, W. J., Arriaga, J., Mangan, B. J., Birks, T. A., & Russell, P. S. J. (2000). *Opt. Lett.*, 25, 1325.
- [14] Steel, M. & Osgood, J. R. M. (2001). *Opt. Lett.*, 26, 229.
- [15] Domanski, A. W. (2005). *Opto-electronic Review*, 13(2), 171.